

Research Article

Cite this article: Koo D, Henderson CA, Askew SD (2024) Agricultural spray drone deposition, Part 1: methods for high-throughput spray pattern analysis. *Weed Sci.* 72: 816–823. doi: [10.1017/wsc.2024.66](https://doi.org/10.1017/wsc.2024.66)

Received: 26 June 2024
Accepted: 31 July 2024
First published online: 29 October 2024

Associate Editor:
William Vencill, University of Georgia

Keywords:
Deposition analysis; droplet size; image analysis; SprayDAT; spray pattern analysis; UAV application

Corresponding author:
Shawn D. Askew; Email: saskew@vt.edu

Agricultural spray drone deposition, Part 1: methods for high-throughput spray pattern analysis

Daewon Koo¹ , Caleb A. Henderson¹  and Shawn D. Askew² 

¹Graduate Research Assistant, School of Plant and Environmental Sciences, Virginia Polytechnic Institute and State University, Blacksburg, VA, USA and ²Professor, School of Plant and Environmental Sciences, Virginia Polytechnic Institute and State University, Blacksburg, VA, USA

Abstract

Effective pesticide application is dependent on precise and sufficient delivery of active ingredients to targeted pests. Water-sensitive papers (WSPs) have been used to estimate the stain coverage, droplet density, droplet size, total spray volume, and other spray-quality metrics by analyzing deposit stains using image analysis software. However, because WSPs are expensive, they are typically distributed along unidimensional transects at intervals of 0.5 m or more, which comprises 0.5% or less of the total treated area. This might limit the ability to accurately represent the deposition of agricultural sprayers with irregular patterns, such as agricultural drone sprayers in the early developmental stage. This study introduces a novel approach utilizing white Kraft paper and a blue colorant proxy for assessing spray deposition. A custom Python-based image analysis tool, SprayDAT (Spray Droplet Analysis Tool), was developed and compared with traditional image analysis software, DepositScan. Both models showed increased accuracy in detecting larger objects, with SprayDAT generally performing better for smaller droplets. DepositScan underestimated the total deposited spray volume by up to 2.7 times less compared with the colorant extraction assessed via spectrophotometry and the predicted output based on flow rate, coverage, and speed. Accuracy of software-estimated spray volume declined with increasing total stain coverage, likely due to overlapping stain objects. Droplet density exhibited a Gaussian trend, with peak density at approximately 22% stain cover, offering evidence for overlapped stains for both DepositScan and SprayDAT as stain cover increased. Both models showed exponential growth in volumetric median diameter (VMD) with increasing stain cover. SprayDAT is freely accessible through an online repository. It features a user-friendly interface for batch processing large sets of scanned images and offers versatility for customization to meet individual needs, such as adjusting spread factor, updating the standard curve for spray volume estimation, or modifying the stain detection threshold.

Introduction

Pesticide efficacy is dependent on the sufficient delivery of active ingredients to targeted pests (Creech et al. 2015; Hislop 1987). According to Knoche (1994), foliar-applied herbicide performance was inversely related to droplet sizes in 71% of 159 experiments. However, small droplets (<100 µm) are prone to drift (Frank et al. 1991), therefore, droplet spectral analysis is used to manage the conflict between pesticide performance and nontarget drift (Al Heidary et al. 2014; Makhnenko et al. 2021; Matthews et al. 2014). With ground-based agricultural sprayers, droplet spectra of a given spray tip are classified under controlled, indoor conditions with high-speed cameras, laser diffraction, or phase doppler particle analysis (Anonymous 2023; Nuyttens et al. 2007; Sijs et al. 2021). Spray tips are then oriented to ensure uniform deposition along the length of an equipment-mounted boom. These systems are designed to deliver inherently uniform spray deposition, so methods employed to assess in-field spray deposition have focused on crop canopy penetration (Chen et al. 2020; Huang et al. 2023; Wang et al. 2019) or wind-mediated drift effects (Fritz et al. 2011; Wang et al. 2020). Because particle analysis systems are impractical for field use, researchers have sought to estimate droplet sizes and overall deposition coverage based on stains deposited on water-sensitive paper (WSP) or other media (Cunha et al. 2012; Fritz et al. 2011; Hewitt et al. 2002; Li et al. 2021a, 2021b; Martin et al. 2019; Panneton 2002; Salyani and Fox 1999; Salyani et al. 2013; Wang et al. 2020; Woldt et al. 2018; Zhu et al. 2011).

There are several limitations in using WSP to assess spray deposition. Most WSP products comprise a sampling area that is less than 30 cm² and are spaced along unidimensional transects at intervals of 0.5 m (Wen et al. 2019; Zhang et al. 2021), 1 m (Ahmad et al. 2020; Qin et al. 2016), or more (Bonds et al. 2023; Fritz et al. 2019). Previously reported research involving WSP-assessed spray deposition sampled between 0.01% and 0.5% of the treated area (Qin et al. 2016;

© The Author(s), 2024. Published by Cambridge University Press on behalf of Weed Science Society of America. This is an Open Access article, distributed under the terms of the Creative Commons Attribution licence (<https://creativecommons.org/licenses/by/4.0/>), which permits unrestricted re-use, distribution and reproduction, provided the original article is properly cited.



Wang et al. 2019). Such discrete sampling may be sufficient for systems with inherently uniform spray delivery but too low to adequately assess deposition uniformity of an agricultural spray drone. However, Richardson et al. (2020) used Gaussian-modeled deposition on steel plates and compared this with modeled deposition estimates based on fluorescence detected on continuous string and found similar slopes across sampling resolutions of 0.25 to 1.0 m. In preliminary research (Koo et al. 2024a, 2024b), our continuous deposition analysis revealed multiple peaks near the center of the spray drone flight path at near 2-m height that were not resolved or reported in the Richardson et al. (2020) paper involving the same model of spray drone. Spray drones are designed to achieve efficient delivery of low-volume spray and typically use rotor-induced wind to disperse small droplets in an effort to increase spray coverage (Qin et al. 2016; Zheng et al. 2018). These design elements are likely to cause changes in deposition patterns depending on drone height and ambient wind (Hunter et al. 2020; Richardson et al. 2020).

Further limitations of WSP are caused by physical characteristics of the bromophenol-blue-coated paper, which vary in response to ambient moisture (Turner and Huntington 1970). Droplets smaller than 50 μm in diameter do not have enough moisture to create stains on WSP (Hoffmann and Hewitt 2005), and small droplet stains that are created may not be resolved by scanners. At relative humidity greater than 85%, WSP stains can increase in size or occur spontaneously (Anonymous 2002; Franz et al. 1998). An overlap of droplet stains can also generate erroneous data, as image analysis software will detect the overlapped droplets as a single droplet. This phenomenon has not been characterized but has been shown to increase with increasing spray volume (Cunha et al. 2012; Zhu et al. 2011). Previous researchers have suggested that utility of WSP to estimate deposition patterns is limited when $\geq 20\%$ of the WSP area is covered by droplet stains (Cunha et al. 2012; Zhu et al. 2011). Ellipse-shaped stains also cause an issue, as image analysis software assumes that droplets have circular shapes to calculate droplet sizes (Deveau 2021b). This is another source of error that will be exacerbated with the advent of agricultural drone sprayers, as these sprayers cause a large percentage of elongated stain objects or streaks due to wind shear (Fritz et al. 2019). Detected objects derived from stains on WSP are identified based on differential hue and saturation, then detected pixel area is converted to an estimated stain diameter assuming all objects are circular (Cunha et al. 2012; Zhu et al. 2011). Estimated stain diameters are converted by a spread factor, specific to each type of WSP (Deveau 2021a), to represent actual droplet size (Ahmad et al. 2020; Anonymous 2002; Cunha et al. 2013; Salyani and Fox 1994, 1999; Zhu et al. 2011).

Given that WSP does not allow for extraction of spray deposits and further estimation of mass per unit area of spray-delivered compounds, relationships of and errors associated with stain coverage on WSP are often limited to relative comparisons that vary by type of WSP (Deveau 2021c) rather than quantifiable deposition. Mylar[®] cards or other plastic- and glass-based samplers are methods that enable pesticide quantification. Spray solutions typically contain dye or fluorescent tracers that are used as a proxy for pesticides. Tracer-treated Mylar[®] cards are removed from the field, washed with ethanol, and analyzed by a spectrofluorometer. The fluorescence value can be converted to a mass dye per area using predetermined standard curves (Fritz et al. 2011; Wang et al. 2020). Much like Mylar[®] cards, extracts of pesticide-sprayed filter papers were analyzed by liquid, gas, or mass chromatography

(Hewitt et al. 2002; Li et al. 2021a, 2021b). Chromatography and fluorometry are robust methods to quantify pesticide delivery, although their costs usually restrict sampling area below that needed to assess highly variable deposition patterns typical of agricultural spray drones. Cotton string and monofilament line also were utilized by researchers using extraction and analysis techniques similar to Mylar[®] card and filter paper assessment (Fritz et al. 2011; Martin et al. 2019; Wang et al. 2020; Woldt et al. 2018). String samplers can generate continuous data, albeit on a narrow, unidimensional transect. This technique is useful for assessing spray drift but not for characterizing multidimensional spray patterns.

Thus, the development of a new analytical method that can characterize spray deposition on continuous and/or multidimensional areas with spatially referenced, mass-to-area assessment of extracted pesticide or tracer dye is needed. Furthermore, assessing accuracy of digitally analyzed stain coverage on paper media to detect droplet deposition quantity and spectral relationships requires spatial reference of stain images and mass-to-area quantification of extracted compounds. To achieve this goal, we utilized spectrophotometric analysis of tracer dye extracted from digitally imaged Kraft paper. A custom Python-based image analysis method, SprayDAT, was compared with the ImageJ-based image analysis software, DepositScan, to estimate total spray deposition and droplet spectral characterization based on actual droplet sizes. SprayDAT offers two advantages over DepositScan that are necessary to deal with the thousands of images generated by continuous sampling of economical Kraft paper. The first is batch processing of images and the second is that code is easily modified depending on the needs of users. To realize these software advantages, SprayDAT must be compared with DepositScan for stain cover and droplet spectral estimation. Because our method allows for both stain imaging and colorant extraction from the same surface, this paper will be the first to report a direct comparison between extracted colorant and digitally analyzed stain objects per unit area. The first objective of this study was to assess the accuracy of digitally imaged stains analyzed by two computer software packages to estimate total spray deposited and droplet spectral characteristics compared with measured spray delivery rates, manufacturer-reported droplet spectral characteristics, and extracted blue colorant quantified via spectrophotometric analysis. Our second objective was to assess the validity of a novel computational method for assessing stain objects as a measure of spray deposition quantity and droplet spectral characterization.

Materials and Methods

Sampler and Proxy

White Kraft paper (Oren International, Pensacola, FL) and colorant (Blazon[®] blue spray pattern indicator, Milliken, Spartanburg, SC) were selected as the sampler and pesticide proxy. This combination provides high-contrast stains like WSP but offers affordable, scalable spatial sampling and easy water extraction and spectrophotometric analysis of the proxy. Because the Kraft paper and dye method costs 0.2 cents for each US\$1 spent on WSP, larger sampling areas are feasible. Preliminary studies were conducted to evaluate various solvents and volumes to assess the extraction efficiency of the proxy colorant. Colorant was extracted from a 528-cm² area of Kraft paper at 99% efficiency (data not shown) using 100 ml of tap water in 125-ml screw-top

jars shaken at 250 rpm with a G2 Gyrotory Shaker (New Brunswick Scientific, Edison, NJ) for 10 min. A 0.4-ml aliquot was removed and mixed with 1.6 ml of tap water, and absorbance was read at 650 nm with a Genesys 5 spectrophotometer (Thermo Fisher Scientific, Waltham, MA). Equation 1 describes the second-order polynomial regression ($R^2 = 0.99$) that relates colorant absorbance value (a) at 650 nm and known amount of colorant (c , μl of colorant 100 ml^{-1} tap water).

$$c = 1.5629a^2 + 10.776a \quad [1]$$

Sample Preparation

Known doses of colorant were applied to 20.3 cm by 30.5 cm Kraft paper using a spray boom equipped with a single flat-fan nozzle (TeeJet® XR11001VS, Spraying Systems, Wheaton, IL) operated at varying speeds at a pressure of 120 kPa, resulting in a flow rate of 4.2 ml s^{-1} . The flow rate and nozzle were selected to mimic the manufacturer-supplied parameters of a DJI MG-1P agricultural spray drone (DJI, Shenzhen, China) that has been evaluated in other experiments. The colorant was mixed 1:1 with water and sprayed in a custom laboratory spray system. A rigid steel frame was prepared to maintain the spray height at 61 cm above the Kraft paper. Four Kraft papers were aligned, and the locations corresponding to the leading and trailing edges of each paper were marked on the steel frame. Thirty unique doses were applied by varying the nozzle speed, which was confirmed via high-speed video (Edgetronic, Sanstreak, Campbell, CA) at $1,500\text{ frames s}^{-1}$. The time required for the spray nozzle to traverse the distance of the paper was measured by the number of frames it was present in the video, and the speed was calculated. As all other factors were held constant, the application volume per unit area and the associated rate of colorant were linearly related to speed. All treated Kraft papers were scanned at 23.6 dots mm^{-1} (600 dpi) with a Ricoh MP C307 color scanner (Ricoh, Tokyo, Japan). Colorant was extracted from a 619-cm^2 area of Kraft paper using 100 ml of tap water in 125-ml screw-top jars shaken at 250 rpm with a G2 Gyrotory Shaker (New Brunswick Scientific) for 10 min. A 0.4-ml aliquot was removed and mixed with 1.6 ml of tap water, and absorbance was read at 650 nm with a Genesys 5 spectrophotometer (Thermo Fisher Scientific).

Development of a New Image Analysis Method, SprayDAT (Spray Droplet Analysis Tool)

Image Conversion

Computational models were generated using Python 3.9 and tested to measure deposition coverage based on colorant stains and to estimate droplet size. Scanned images were converted to grayscale images, and a selected threshold of 154 within the grayscale range of 0 to 255 was applied to create a binary mask of black droplet stains and white backgrounds. The threshold was found to best encompass all of the detected droplets without highlighting potential noise in the scanned images, such as dust or dirt particles. The outline of each stain was detected using the contour detection algorithm proposed by Suzuki and Abe (1985), and the areas of each stain were calculated based on Green's theorem (Marsden and Tromba 2003). Each stain was then considered to be a circle, and the diameter of each stain was estimated. The proportion of stain area and the number of stain objects were used to calculate spray coverage and droplet density, respectively.

Reference Stain Detection

To test the accuracy of stain detection by SprayDAT, nominal spot sizes of 100, 200, 300, 500, 1,000, and 2,000 μm in diameter on the reference card (ORBITRANSIT, Shanghai, China) were analyzed. The reference card was scanned at 23.6 dots mm^{-1} (600 dpi) using a Ricoh MP C307 color scanner (Ricoh). The diameters of the nominal-sized spots on the scanned images were analyzed by SprayDAT and compared with the DepositScan results.

Spread Factor

To estimate the actual droplet sizes from the Kraft paper sampler, the spread factor between the stain size and actual droplet sizes needed to be determined (Cunha et al. 2012, 2013; Zhu et al. 2011). The spread factor between Kraft paper and blue colorant, which has not been reported by previous researchers, was determined across a range of discrete droplet diameters, using methods similar to those of Smith et al. (2000). A custom-built droplet generator consisting of a 2.5-cm spinning disk was operated via a brushless motor at 3,750 rpm. Droplets of discrete size were ejected through a 0.5 cm by 1.0 cm aperture in an enclosure around the spinning disk at 46 cm above the sampling location. A camera slider (GVM GT-60D, Great Video Maker, Philadelphia, PA) was fit with a horizontal platform that contained a 5-cm petri dish filled with a biphasic solution of polydimethylsiloxane (PDMS) (MicroLubrol®, Type 200 Silicone Oil, MicroLubrol, Clifton, NJ), and a 25-cm^2 sheet of Kraft paper. The lower 1 mm of the dish contained PDMS of 12,500 cSt viscosity, while the upper 2 mm layer contained PDMS of 100 cSt viscosity. Droplets are suspended in the oil solution at the interface between the two PDMS layers of varying viscosity, allowing for accurate imaging on a narrow plane. Both PDMS-filled petri dishes and Kraft papers were placed 20, 32, 43, 55, 66, 77, and 89 cm from the droplet generator to achieve droplet diameters of 112, 143, 183, 218, 246, 275, and 315 μm , respectively, with a standard deviation less than 10% in all cases.

After treatment with different-sized droplets, the petri dishes were carefully transferred to a white translucent panel illuminated underneath with an LED light (Craftsman® 4500LM 46W LED Work Light, Craftsman, Towson, MD) and photographed with a digital camera (Canon EOS 5D, Canon, Tokyo, Japan) at an effective resolution of 157 dots mm^{-1} (2,400 dpi). Kraft papers were scanned at 23.6 dots mm^{-1} (600 dpi) with a Ricoh MP C307 color scanner (Ricoh). The droplet sizes and stain diameters were measured by counting pixels and were converted based on known pixel to distance relationships using the binarization threshold of 154 within the grayscale range of 0 to 255. The spread factor was calculated as the difference between droplet diameters in the PDMS solution and stain diameters on Kraft paper.

Droplet Spectra Analysis

A total of 120 scanned sample images were digitally analyzed via SprayDAT and compared with analyses from ImageJ-based DepositScan software developed by USDA-ARS (Zhu et al. 2011). Detected droplet stains on each scanned image were converted to actual droplet sizes based on the calculated spread factor. Afterwards, the volume of each droplet was calculated based on Equation 2, where V_i is the estimated droplet volume and d_i is the estimated droplet diameter.

$$V_i = \frac{\pi d_i^3}{6}, \quad i = 1, \dots, N \quad [2]$$

Cumulative volume was calculated by summing the volume of each droplet, and $D_{v0.1}$, $D_{v0.5}$ (VMD), and $D_{v0.9}$ were calculated using an interpolation method similar to that described by Zhu et al. (2011). Because DepositScan generates $D_{v0.1}$, VMD, and $D_{v0.9}$ based on a spread factor ($d = 0.95 d_s^{0.910}$) originating from work on WSP, output from DepositScan was adjusted using the Kraft paper-specific spread factor described in Equation 3.

Spray Deposition Estimation

In addition to comparing computational models for droplet spectra, we assessed the total deposition of blue colorant from different computational models. First, the reference spray deposition was estimated based on the application speed of each sample, as the spray volume could be calculated from the known flow rate and spray width. An extraction-based method was also employed to quantify total colorant extracted from each piece of Kraft paper that could then be used to quantify spray deposition. This method utilized a standard curve correlating colorant dosage with spectrophotometric absorbance values, which were then converted into deposition volumes (μl colorant cm^{-2}), accounting for the surface area of the sample. The colorant deposited per unit area estimated by SprayDAT or DepositScan was based on the total volume of all droplets based on measurements of each discrete stain object via digital imagery of sprayed Kraft paper adjusted for the ratio of colorant to water.

Results and Discussion

Spread Factor Calculation

The difference between droplet diameters in the PDMS solution and stain diameters on Kraft paper were subjected to a nonlinear two-parameter power regression ($R^2 = 0.9$) where d_s and d are stain and actual droplet diameters (in μm), respectively.

$$d = 0.83d_s^{0.79} \quad [3]$$

Compared with the spread factor ($d = 0.95 d_s^{0.910}$) of the WSP described in Zhu et al. (2011), Equation 3 indicated that blue colorant proxy left more stains on white Kraft paper than water on the WSP.

Object Detection and Measurement by Two Computational Models

Table 1 describes the trend of object detection when two computational models (SprayDAT and DepositScan) assessed objects of known nominal sizes ranging from 100 to 2000 μm on reference cards (ORBITTRANSIT). Both SprayDAT and DepositScan exhibited a trend of increased accuracy in diameter detection as object size increased (Table 1), as has been reported for similar object size estimation (Brandoli et al. 2021; Zhu et al. 2011). SprayDAT enlarged 100- μm droplets by 17%, but all other objects were measured accurately to within a 4% error rate. DepositScan, in contrast, enlarged 100-, 200-, and 300- μm objects 51%, 22%, and 10%, respectively, while accurately measuring objects that were 500 to 2,000 μm within a 5% error rate. When 120 Kraft paper samples were analyzed for spray deposition stains, total cover of all stain objects estimated by DepositScan and SprayDAT were linearly

Table 1. Comparison of diameters measured by SprayDAT and DepositScan for nominal spot diameters of 100, 200, 300, 400, 500, 1,000, and 2,000 μm on a size reference card.^a

Nominal diameter	Determined by SprayDAT		Determined by DepositScan	
	Diameter	Difference	Diameter	Difference
μm	μm	%	μm	%
100	117	17.01	151	51.06
200	208	4.11	243	21.79
300	292	2.49	331	10.32
400	385	3.72	422	5.47
500	489	2.10	528	5.52
1,000	991	0.95	1,029	2.90
2,000	1,999	0.04	2,037	1.86

^aThe reference card (ORBITTRANSIT, China) was scanned at 23.6 dots mm^{-1} with the Ricoh MP C307 color scanner (Ricoh, Tokyo, Japan).

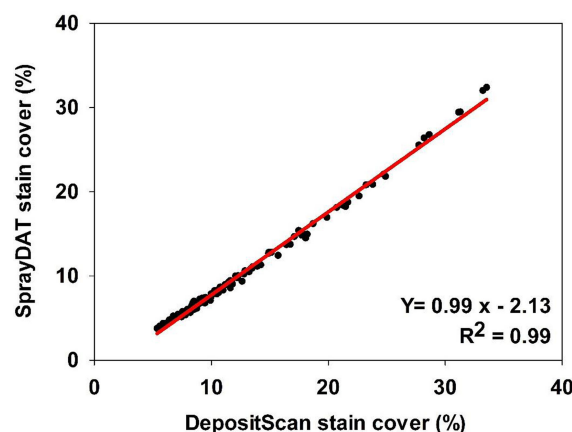


Figure 1. The relationship between percentage stain cover of 120 scanned Kraft paper samples assessed using SprayDAT and DepositScan.

related with a 0.99 coefficient of determination (Figure 1). The slope of 0.99 that relates total stain cover between the computational models indicates that SprayDAT is estimating stain objects to be slightly smaller compared with DepositScan (Figure 1), in agreement with observations made when estimating known objects on reference cards, where DepositScan enlarged objects as much as 51% (Table 1). Across the 120 Kraft paper samples sprayed in the laboratory, application speeds ranged from 0.4 to 8.4 m s^{-1} , resulting in 3.8% to 33.4% SprayDAT-assessed stain cover (Figure 2). The relationship between application speed and percentage stain cover followed an inverse first-order polynomial regression ($R^2 = 0.95$) and deviated only slightly in trend from predicted application volume based on variable speeds given a constant flow rate of 4.2 ml s^{-1} (Figure 2).

Droplet Density Relationships

The density of individual stain objects on Kraft paper is referred to as “droplet density” and is expressed as the estimated number of droplets landing in each square centimeter of Kraft paper. The relationship of droplet density as measured by SprayDAT and DepositScan was linear with a 0.93 coefficient of determination. The slope of 1.13 indicates that SprayDAT is estimating a higher number of droplets per unit area compared with DepositScan (Figure 3). The likely reason for increased droplet density assessed

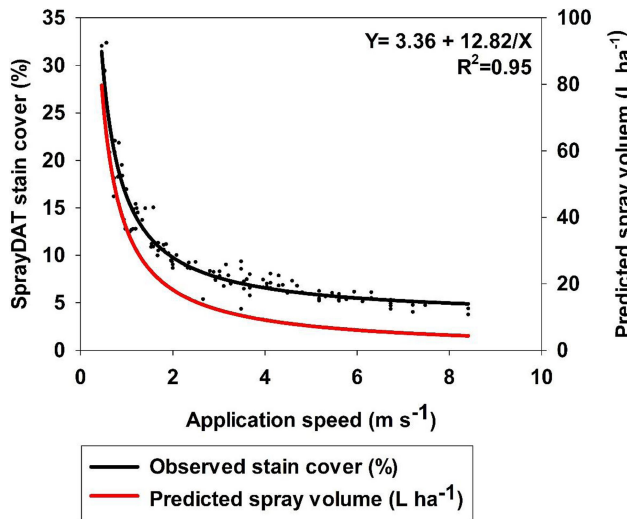


Figure 2. The relationship between the application speed and SprayDAT-assessed stain cover on 120 scanned Kraft paper samples. Predicted spray volume as calculated based on constant flow rate and variable speed is provided as a reference.

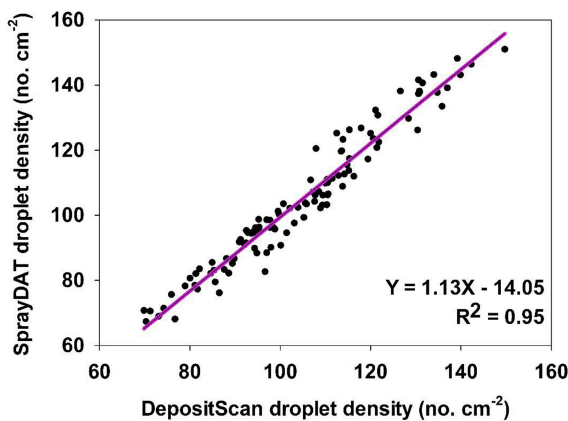


Figure 3. The relationship between droplet density (droplets cm^{-2}) of 120 scanned Kraft paper samples assessed using SprayDAT and DepositScan.

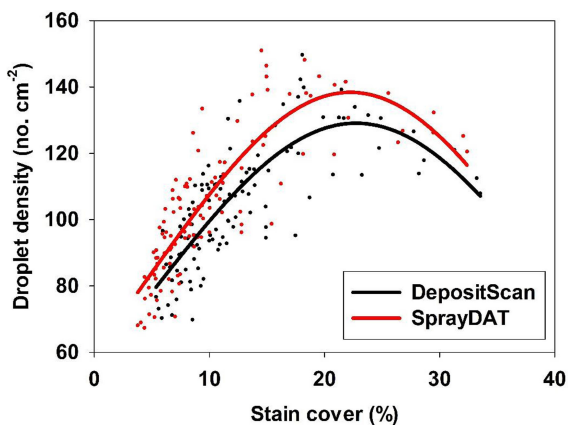


Figure 4. The relationship between percentage stain cover and droplet density (droplets cm^{-2}) of 120 scanned Kraft paper samples assessed using SprayDAT and DepositScan.

Table 2. Volume median diameter (VMD; $Dv_{0.5}$), $Dv_{0.1}$ and $Dv_{0.9}$ measured by ImageJ-based DepositScan and Python-based SprayDAT for stain objects detected on 120 Kraft paper samples following spray of a blue colorant solution.^a

Image analysis method	VMD ($Dv_{0.5}$)	$Dv_{0.1}$	$Dv_{0.9}$
	μm		
DepositScan ^b	325 A	180 A	562 A
DepositScan with spread factor correction ^c	121 B	76 B	191 B
SprayDAT	108 C	63 C	178 B
SprayDAT bounded 40 to 300 μm	106 C	63 C	170 B
SprayDAT bounded 40 to 400 μm	107 C	64 C	175 B

^aOriginal DepositScan output was compared with output with an adjusted spread factor, and SprayDAT was executed with or without bounding to exclude objects smaller than 40 μm or larger than 300 to 400 μm that were deemed erroneous. All samples were scanned at 23.6 dots mm^{-1} with a Ricoh MP C307 color scanner (Ricoh, Tokyo, Japan). Means within a given column followed by the same letter are not different according to Fisher's Protected LSD ($\alpha = 0.05$).

^bOriginal software uses a spread factor to relate stain size to estimated droplet size based on work with water-sensitive paper.

^cSpread factor (Equation 2) was adjusted to reflect relationship between blue stains on Kraft paper and actual size of droplets suspended in oil solution.

by SprayDAT is the higher accuracy of SprayDAT in detecting smaller droplets (Table 1). Detecting overlapping multiple droplets as a single large droplet has been a widely reported problem in image analysis techniques for paper-based samplers such as WSPs (Brandoli et al. 2021; JPAR Cunha et al. 2013; M Cunha et al. 2012; Fox et al. 2003; Özlüoymak and Bolat 2020; Zhu et al. 2011), but none of these reports characterized the relationship between total stain cover and droplet density. In our study, the number of unique stain objects exhibited a Gaussian trend as total stain cover increased with peak droplet densities of 129 and 138 droplets cm^{-2} for DepositScan and SprayDAT, respectively (Figure 4). These peak droplet densities were reached at 22.7% and 22.2% stain cover, respectively, after which, droplet density declined (Figure 4). The decline in droplet density after 22% stain cover is evidence that additional droplet stains increasingly overlap as more droplets are added. These overlapping stains either merge into larger stain formations or are concealed by preexisting stains, resulting in a complex pattern of layered stains. This phenomenon was reported but not characterized by other researchers (Brandoli et al. 2021; Fox et al. 2003; Zhu et al. 2011). Fox et al. (2003) estimated arbitrarily that WSPs or Kromekote[®] cards with stain coverage exceeding 20% would be of limited value for estimating total volume of spray per unit area. This 20% estimate aligns well with our Gaussian relationship between total stain coverage and droplet density (Figure 4). While neither computational method can resolve overlapping stain objects, SprayDAT tended to more accurately detect small stains (Table 1) and slightly conserve droplet density (Figures 3 and 4) compared with DepositScan.

Estimating Droplet Spectra Based on Stain Objects

The average VMD estimated by SprayDAT and spread factor-corrected (Equation 3) DepositScan across 120 Kraft papers sprayed at a constant flow rate with variable speed was 108 μm and 121 μm , respectively (Table 2). The manufacturer of the Teejet[®] XR11001VS nozzle characterizes the spray output at the utilized operating pressure of 120 kPa (Anonymous 2023) as "Fine" based on the American Society of Agricultural and Biological Engineers (ASABE) Standard 572.3, suggesting the VMD ranges from 106 to

Table 3. Nonlinear regression equations with parameters utilized for this study.

Figure	Model	Equation name	Equation	Parameters	R ²
4	SprayDAT	Gaussian	$y = y_0 + ae^{-0.5(x-x_0)/b^2}$	$a = 138, b = 17.3, x^0 = 22.2$	0.73
4	DepositScan	Gaussian	$y = y_0 + ae^{-0.5(x-x_0)/b^2}$	$a = 129, b = 17.7, x^0 = 22.7$	0.64
5	DepositScan	Exponential growth	$y = ae^{(bx)}$	$a = 170.06,$ $b = 0.0456$	0.97
5	DepositScan adjusted	Exponential growth	$y = ae^{(bx)}$	$a = 75.38,$ $b = 0.034$	0.97
5	SprayDAT	Exponential growth	$y = ae^{(bx)}$	$a = 68.6,$ $b = 0.039$	0.98
6	Speed estimation	Power	$y = ax^b$	$a = 0.0051,$ $b = 1.263$	0.94
6	Extraction	Power	$y = ax^b$	$a = 0.0045,$ $b = 1.279$	0.99
6	Stain object–DepositScan	Power	$y = ax^b$	$a = 0.0014,$ $b = 1.259$	0.99
6	Stain object–SprayDAT	Power	$y = ax^b$	$a = 0.0009,$ $b = 1.348$	0.99

Description of equations used

Gaussian $y = y_0 + ae^{-0.5(x-x_0)/b^2}$, where y is the droplet density (droplet cm^{-2}), a is the peak height, b is the width of the peak, x is the percentage stain cover assessed by image analysis software, x^0 is the center or mean of the peak, and y_0 is the offset.

Exponential growth $y = ae^{(bx)}$, where y is volume median diameter (VMD, μm), a is the lower asymptote, b is the growth rate parameter, and x is the percentage stain cover assessed by image analysis software.

Power $y = ax^b$, where y is total blue colorant deposition ($\mu\text{l cm}^{-2}$), a is the scaling factor, b is the growth rate parameter, and x is the percentage stain cover assessed by image analysis software.

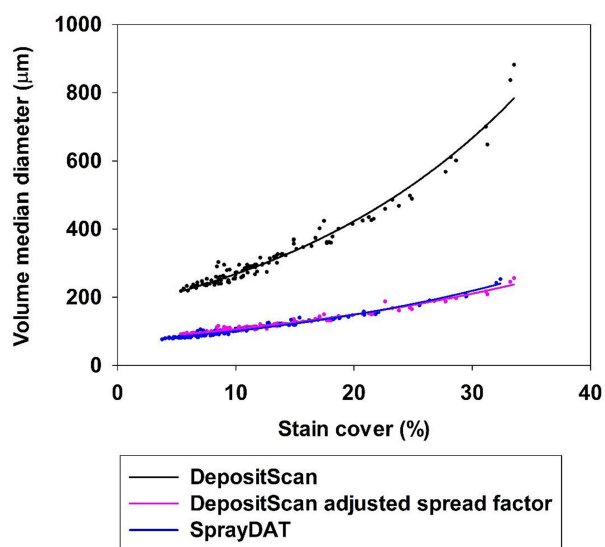


Figure 5. The relationship between the percentage stain cover and volume median diameter (μm) of 120 scanned Kraft paper samples assessed by DepositScan, DepositScan with adjusted spread factor, and SprayDAT.

235 μm (Anonymous 2020; Grisso et al. 2019). Therefore, average VMD estimations from SprayDAT and DepositScan with adjusted spread factor were in the range of expected values, although DepositScan estimated a significantly larger VMD compared with SprayDAT. Excluding objects that were outside the bounds of 40 to 300 μm or 40 to 400 μm did not significantly impact VMD, $DV_{0.1}$, or $DV_{0.9}$ (Table 2).

The data in Table 2 appear to contrast with reports of overlapping and enlarged stain objects as total stain coverage increases (Brandoli et al. 2021; Fox et al. 2003; Zhu et al. 2011), as bounding did not alter VMD estimation by SprayDAT (Table 2). It should be noted, however, that more than 60% of our 120 Kraft paper samples had total stain coverage of less than 10%, and only 11 of the 120 samples exceeded total stain coverage of 20% (Figure 2). Thus, our average spectral analysis across all 120

samples was less subject to the errors associated with excessive total stain coverage. When we evaluate VMD as a function of total stain cover, the data fit an exponential growth curve (Table 3, Figure 5) in all cases for DepositScan, DepositScan with adjusted spread factor, and SprayDAT. Because all factors were held constant, with the exception of speed, the VMD in this laboratory experiment should be constant. The increase in VMD associated with increased stain cover in the computational models is evidence of overlapping or merged deposition stains that occur in increasing frequency as total stain cover increases. The data in Figure 3 also highlight the importance of spread factor accuracy. The original output from DepositScan is largely deviant compared with SprayDAT or spread factor–adjusted DepositScan. Because spread factors have been reported to deviate with varying WSP products (Deveau 2021a), we see this as a significant limitation of DepositScan. The method required to adjust DepositScan output as spread factor changes (Zhu et al. 2011) requires numerous manual calculations with limited ability for automation. In SprayDAT, images are batch processed, and users would simply replace one equation at a specified place in the code if a different spread factor were desired.

Accuracy of Predicting Deposition Volume via Spray Deposit Stains

Despite numerous papers evaluating WSP or other methods to digitally assess spray deposit stains (Brandoli et al. 2021; Cunha et al. 2012, 2013; Ferguson et al. 2016; Özlüoymak and Bolat 2020; Zhu et al. 2011) and spray volume per unit area estimates based on deposit stains computed by available software (Brandoli et al. 2021; Zhu et al. 2011), the accuracy of spray volume estimates based on stain object-to-droplet volume relationships remains unreported. A nonlinear two-parameter power model described the relationship between total stain cover on Kraft paper and estimated spray volume deposited based on speed and flow rate of the sprayer, extracted colorant quantified by standardized spectrophotometric absorbance, and deposit stains measured by DepositScan or SprayDAT (Figure 6). The extraction method underestimated spray deposition approximately 9% compared with speed-based

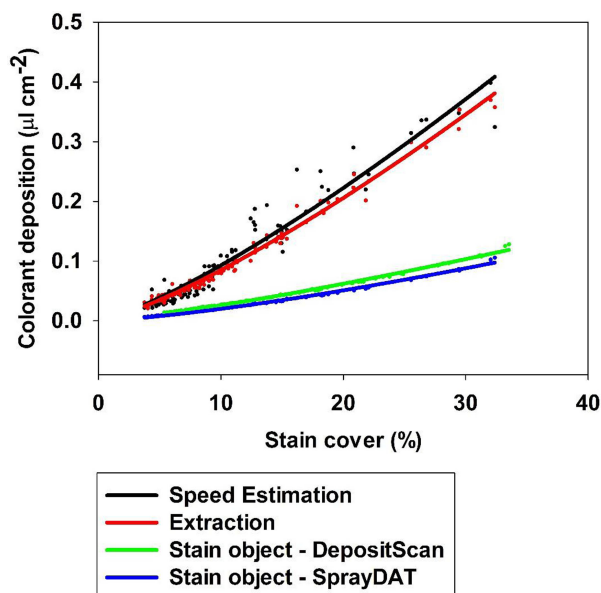


Figure 6. The relationship between percentage stain cover and estimated total colorant deposited ($\mu\text{l cm}^{-2}$) predicted by speed calculation, colorant extraction, and stain object-based volume calculated using SprayDAT and DepositScan.

calculations, which are considered the reference (Figure 6). The underestimation might be attributed to losses during the extraction process, but preliminary experiments indicate our extraction method accounts for more than 99% of colorant (data not shown).

Both computational models that relied on deposit stains were divergent with the actual predicted spray volume of calibrated equipment and estimates of spray volume based on extracted colorant. The divergence between these methods increased with increasing total stain cover, such that DepositScan and SprayDAT estimated 2.7 and 3.2 times less spray volume than speed-based predictions when total stain coverage was 30% (Figure 6). The complementary trends among all four methods is testament that estimates based on stain objects can appropriately reflect relative differences in spray deposition, but these data are the first to characterize how inaccurately deposit stain-based methods estimate spray volume compared with colorant extraction or predicted spray output based on equipment calibration. This inaccuracy likely stems from declining droplet density as total stain coverage increases (Figure 4), a problem inherent to estimates based on deposit stains. When the x axis of Figure 4 was truncated to 10% total stain cover, a linear trend ($R^2 = 0.97$) with slope 13.2 was predicted (data not shown). If this early linear trend is extrapolated to 30% total stain cover, droplet density would be estimated at $397 \text{ drops cm}^{-2}$, or three times greater than that detected by digital image analysis and similar to the disparity between extracted colorant and model-predicted colorant deposition (Figure 6). Future efforts will use artificial intelligence to better estimate how congregated stain objects may be separated for more accurate deposition assessments.

Acknowledgments. The authors would like to acknowledge Clebson G. Gonçalves of UC Agricultural and Natural Resources for technical assistance for this project.

Funding statement. This research received no specific grant from any funding agency or the commercial or not-for-profit sectors.

Competing interests. The authors declare no conflicts of interest.

References

- Ahmad F, Qiu B, Dong X, Ma J, Huang X, Ahmed S, Chandio FA (2020) Effect of operational parameters of UAV sprayer on spray deposition pattern in target and off-target zones during outer field weed control application. *Comput Electron Agric* 172:105350
- Al Heidary M, Douzals JP, Sinfort C, Vallet A (2014) Influence of spray characteristics on potential spray drift of field crop sprayers: a literature review. *Crop Prot* 63:120–130
- Anonymous (2002) Water-Sensitive Paper for Monitoring Spray Distributions. Basel: Syngenta Crop Protection AG. 8 p
- Anonymous (2020) Spray Nozzle Classification by Droplet Spectra. Standard 572.3. St Joseph, MI: American Society of Agricultural and Biological Engineers. 5 p
- Anonymous (2023) TeeJet Technologies Catalog 52. Wheaton, IL: Spraying Systems Co. 204 p
- Bonds JA, Fritz B, Thistle HW (2023) Calculation of swath width and swath displacement for uncrewed aerial spray systems. *J ASABE* 66:523–532
- Brandoli B, Spadon G, Esau T, Hennessy P, Carvalho AC, Amer-Yahia S, Rodrigues-Jr JF (2021) DropLeaf: a precision farming smartphone tool for real-time quantification of pesticide application coverage. *Comput Electron Agric* 180:105906
- Chen P, Lan Y, Douzals JP, Ouyang, F, Wang J, Xu W (2020) Droplet distribution of Unmanned Aerial Vehicle under several spray volumes and canopy heights in the cotton canopy. *Int J Precis Agric Aviat* 3(4):74–79
- Cunha M, Carvalho C, Marcal AR (2012) Assessing the ability of image processing software to analyse spray quality on water-sensitive papers used as artificial targets. *Biosyst Eng* 111:11–23
- Cunha JPAR, Farnese AC, Olivet JJ (2013) Computer programs for analysis of droplets sprayed on water sensitive papers. *Planta Daninha* 31:715–720
- Creech CF, Henry RS, Werle R, Sandell LD, Hewitt AJ, Kruger GR (2015) Performance of postemergence herbicides applied at different carrier volume rates. *Weed Technol* 29:611–624
- Deveau J (2021a) Assessing Water Sensitive Paper—part 1. https://sprayers101.com/assessing_wsp_pt1. Accessed: April 18, 2023
- Deveau J (2021b) Assessing Water Sensitive Paper—part 3. https://sprayers101.com/assessing_wsp_pt3. Accessed: April 18, 2023
- Deveau J (2021c) Comparing Three Brands of Water Sensitive Paper. https://sprayers101.com/3_wsp. Accessed: April 18, 2023
- Ferguson JC, Chechetto RG, O'Donnell CC, Fritz BK, Hoffmann WC, Coleman CE, Chauhan BS, Adkins SW, Kruger GR, Hewitt AJ (2016) Assessing a novel smartphone application—SnapCard, compared to five imaging systems to quantify droplet deposition on artificial collectors. *Comput Electron Agric* 128:193–198
- Fox RD, Derksen RC, Cooper JA, Krause CR, Ozkan HE (2003) Visual and image system measurement of spray deposits using water-sensitive paper. *Appl Eng Agric* 19:549
- Frank R, Johnson K, Braun HE, Halliday CG, Harvey J (1991) Monitoring air, soil, stream and fish for aerial drift of permethrin. *Environ Monit Assess* 16:137–150
- Franz E, Bouse LF, Carlton JB, Kirk IW, Latheef MA (1998) Aerial spray deposit relations with plant canopy and weather parameters. *Trans ASAE* 41:959–966
- Fritz B, Gill M, Brettbauer S (2019) Examining aerial application swath pattern evaluations under in-wind and cross-wind conditions. Pages 24–38 in *Proceedings of the 39th Symposium on Pesticide Formulation and Delivery Systems: Innovative Formulation, Application and Adjuvant Technologies for Agriculture*. Washington, DC: ASTM International
- Fritz BK, Hoffmann WC, Bagley WE, Hewitt A (2011) Field scale evaluation of spray drift reduction technologies from ground and aerial application systems. *J ASTM Int* 8:1–11
- Grisso RD, Askew SD, McCall DS (2019) Nozzles: selection and sizing. Virginia Cooperative Extension, 12 p
- Henderson C, Koo D, Askew S (2024) SprayDAT. Software. University Libraries, Virginia Tech. <https://doi.org/10.7294/25403470>
- Hewitt AJ, Johnson DR, Fish JD, Hermansky CG, Valcore DL (2002) Development of the spray drift task force database for aerial applications. *Environ Toxicol Chem* 21:648–658.
- Hislop EC (1987) Can we define and achieve optimum pesticide deposits? *Asp Appl Biol* 14:153–172

- Hoffmann WC, Hewitt AJ (2005) Comparison of three imaging systems for water-sensitive papers. *Appl Eng Agric* 21:961–964
- Huang Z, Wang C, Wongsuk S, Qi P, Liu L, Qiao B, Zhong L, He X (2023) Field evaluation of a six-rotor unmanned agricultural aerial sprayer: effects of application parameters on spray deposition and control efficacy against rice planthopper. *Pest Manag Sci* 79:4664–4678
- Hunter JE, Gannon TW, Richardson RJ, Yelverton FH, Leon RG (2020) Coverage and drift potential associated with nozzle and speed selection for herbicide applications using an unmanned aerial sprayer. *Weed Technol* 34:235–240
- Knoche M (1994) Effect of droplet size and carrier volume on performance of foliage-applied herbicides *Crop Prot* 13:163–178
- Koo D, Godara N, Romero Cubas JR, Askew SD (2024a) A method to spatially assess multipass spray deposition patterns via UV-fluorescence and weed population shifts. *Crop Sci* 1–12. <https://doi.org/10.1002/csc2.21377>
- Koo D, Henderson CA, Askew SD (2024b) Agricultural spray drone deposition, Part 2: operational height and nozzle influence pattern uniformity, drift, and weed control. *Weed Sci* 1–9. <https://doi.org/10.1017/wsc.2024.67>
- Li X, Giles DK, Andaloro JT, Long R, Lang EB, Watson LJ, Qandah I (2021a) Comparison of UAV and fixed-wing aerial application for alfalfa insect pest control: evaluating efficacy, residues, and spray quality. *Pest Manag Sci* 77:4980–4992
- Li X, Giles DK, Niederholzer FJ, Andaloro JT, Lang EB, Watson LJ (2021b) Evaluation of an unmanned aerial vehicle as a new method of pesticide application for almond crop protection. *Pest Manag Sci* 77:527–537
- Makhnenko I, Alonzi ER, Fredericks SA, Colby CM, Dutcher CS (2021) A review of liquid sheet breakup: perspectives from agricultural sprays. *J Aerosol Sci* 157:105805
- Marsden JE, Tromba A (2003) *The Integral Theorems of Vector Analysis. Vector calculus (5th ed.)*. New York: W.H. Freeman. 518–608 pp. ISBN 978-0-7167-4992-9
- Martin DE, Woldt WE, Lathief MA (2019) Effect of application height and ground speed on spray pattern and droplet spectra from remotely piloted aerial application systems. *Drones* 3:83
- Matthews G, Bateman R, Miller P (2014) *Pesticide Application Methods*. Hoboken, NJ: Wiley. 503 p
- Nuytens D, Baetens K, De Schampheleire M, Sonck B (2007) Effect of nozzle type, size and pressure on spray droplet characteristics. *Biosyst Eng* 97:333–345
- Özlüoymak ÖB, Bolat A (2020) Development and assessment of a novel imaging software for optimizing the spray parameters on water-sensitive papers. *Comput Electron Agric* 168:105104
- Panneton B (2002) Image analysis of water-sensitive cards for spray coverage experiments. *Appl Eng Agric* 18:179
- Qin WC, Qiu BJ, Xue XY, Chen C, Xu ZF, Zhou QQ (2016) Droplet deposition and control effect of insecticides sprayed with an unmanned aerial vehicle against plant hoppers. *Crop Prot* 85:79–88
- Richardson B, Rolando CA, Somchit C, Dunker C, Strand TM, Kimberley MO (2020) Swath pattern analysis from a multi-rotor unmanned aerial vehicle configured for pesticide application. *Pest Manag Sci* 76:1282–1290
- Salyani M, Fox RD (1994) Performance of image analysis for assessment of simulated spray droplet distribution. *Trans ASAE* 37:1083–1089
- Salyani M, Fox RD (1999) Evaluation of spray quality by oil and water-sensitive papers. *Trans ASAE* 42:37–43
- Salyani M, Zhu H, Sweeb RD, Pai N (2013) Assessment of spray deposition with water-sensitive paper cards. *Agric Eng Int CIGR J* 15:101–111
- Sijts R, Kooij S, Holterman HJ, Van De Zande J, Bonn D (2021) Drop size measurement techniques for sprays: comparison of image analysis, phase Doppler particle analysis, and laser diffraction. *AIP Adv* 11:015315
- Smith DB, Askew SD, Morris WH, Shaw DR, Boyette M (2000) Droplet size and leaf morphology effects on pesticide spray deposition. *Trans ASAE* 43:255
- Suzuki S, Abe K (1985) Topological structural analysis of digitized binary images by border following. *Lect Notes Comput Sc* 30:32–46
- Turner CR, Huntington KA (1970) The use of a water sensitive dye for the detection and assessment of small spray droplets. *J Agric Eng Res* 15:385–387
- Wang G, Han Y, Li X, Andaloro J, Chen P, Hoffmann WC, Han X, Chen S, Lan Y (2020) Field evaluation of spray drift and environmental impact using an agricultural unmanned aerial vehicle (UAV) sprayer. *Sci Total Environ* 737:139793
- Wang G, Lan Y, Qi H, Chen P, Hewitt A, Han Y (2019) Field evaluation of an unmanned aerial vehicle (UAV) sprayer: effect of spray volume on deposition and the control of pests and disease in wheat. *Pest Manag Sci* 75:1546–1555
- Wen Y, Zhang R, Chen L, Huang Y, Yi T, Xu G, Li L, Hewitt AJ (2019) A new spray deposition pattern measurement system based on spectral analysis of a fluorescent tracer. *Comput Electron Agric* 160:14–22
- Woldt W, Martin D, Lahteef, M, Kruger G, Wright R, McMechan J, Proctor C, Jackson-Ziems T (2018) Field evaluation of commercially available small unmanned aircraft crop spray systems. *In 2018 ASABE Annual International Meeting*. St Joseph, MI: American Society of Agricultural and Biological Engineers. <https://doi.org/10.13031/aim.201801143>
- Zhang P, Zhang W, Sun HT, He FG, Fu HB, Qi LQ, Yu LJ, Jin LY, Zhang B, Liu JS (2021) Effects of Spray Parameters on the Effective Spray Width of Single-Rotor Drone in Sugarcane Plant Protection. *Sugar Technol* 23:308–315
- Zheng Y, Yang S, Liu X, Wang J, Norton T, Chen J, Tan Y (2018) The computational fluid dynamic modeling of downwash flow field for a six-rotor UAV. *Front Agric Sci Eng* 5:159–167
- Zhu H, Salyani M, Fox RD (2011) A portable scanning system for evaluation of spray deposit distribution. *Comput Electron Agric* 76:38–43